Eur J Plant Pathol (2010) 128:473–482
DOI 10.1007/s10658-010-9674-1

Temporal and spatial dynamics of watermelon gummy stem blight epidemics

Adalberto C. Café-Filho · Gil R. Santos · Francisco F. Laranjeira

Accepted: 5 August 2010 / Published online: 31 August 2010

Abstract The effect of the distance of initial inoculum on the intensity of watermelon gummy stem blight, caused by *Didymella bryoniae*, was studied in a naturally-infected rainfed commercial field. The shorter the distance from the focus, the sooner was disease onset and the earlier maximum disease levels were achieved. Maximum disease incidences were reached earlier than maximum severities, but eventually destructive levels were observed for both disease incidence and severity. Disease progressed at similar rates, irrespective of the radial distance from the focus. A detailed study of the disease temporal progress was conducted in inoculated rainfed experimental fields with commercial genotypes Crimson Sweet (susceptible, S) and Riviera (moderately resistant, R). The Gompertz model best described the disease progress curves, and estimated apparent infection rates were 0.049 and 0.020 respectively for S and R genotypes. In addition, spatial pattern studies were conducted during the dry season in overhead irrigated experimental plots, inoculated with point-source foci. Disease intensity gradients were better explained by the Exponential model than by the Power Law model. Gummy stem blight distribution was classified as aggregated by the Ordinary Runs procedure. Two different spatial autocorrelation methods (2DCorr and LCOR) revealed strong short distance spatial dependencies. Long distance positive correlations between quadrats were observed along with periods of higher progress rates. The dynamic patterns of the epidemics of gummy stem blight in watermelon described here are consistent with epidemics of polycyclic diseases with splash-dispersed spores.

Keywords *Didymella bryoniae* · *Ascochyta cucumis* · *Phoma cucurbitacearum* · *Citrullus lanatus*

A. C. Café-Filho (✉)
Departamento de Fitopatologia, Universidade de Brasília,
70910-900 Brasília, DF, Brazil
e-mail: cafefilh@unb.br

G. R. Santos
Departamento de Agronomia,
Universidade Federal do Tocantins,
77402-970 Gurupi, TO, Brazil

F. F. Laranjeira
Embrapa Mandioca e Fruticultura,
44380-000 Cruz das Almas, BA, Brazil

Introduction

Gummy stem blight (GSB), caused by *Didymella bryoniae* (Auersw) Rehm (= *Mycosphaerella citrullina* (C.O.Sm.) Gross.), anamorph *Ascochyta cucumis* Fautrey & Roum (=*Phoma cucurbitacearum* (Fr.:Fr.) Sacc.), is one of the most important diseases of watermelon (*Citrullus lanatus* (Thunb.) Matsum. and Nakai) and other Cucurbitaceae (Keinath 1995).

Disease symptoms include stem canker, foliar blight and fruit rot (Schenck 1968). Losses due to *D. bryoniae* vary from 17% (Keinath et al. 1997) to 43% (Keinath and Duthie 1998). Santos et al. (2005) detected a highly negative correlation (r=−0.96) between foliar blight levels and fruit yield and found a 19.2% yield loss due to GSB. In spite of its importance, the disease´s temporal and spatial dynamics have not been described. Temporal and spatial analysis of plant disease epidemics have been carried out for several pathosystems (Madden and Hughes 1995) and have even helped to elucidate the disease aetiology (Fajardo et al. 1997; Laranjeira et al. 1998). The interpretation of disease progress and disease gradient curves provides a better understanding of epidemic processes in the field (Campbell and Madden 1990), and this understanding may allow for better management of GSB epidemics. Spatial studies have been done by a range of methods, including disease gradient modelling, joint-count statistics and spatial autocorrelation (Berger and Luke 1979; Ferrandino 1998; Gottwald and Graham 1990; Maffia and Berger 1999; Madden et al. 2007). Since no such studies have been reported on gummy stem blight, this work aimed to describe its temporal and spatial dynamics in experimental or commercial fields.

Materials and methods

Effect of inoculum source distance on GSB progress in rainfed watermelon

The temporal progress of GSB from 10 naturally occurring, randomly distributed foci was monitored between October and December 2003 in a rainfed, commercial field untreated with fungicides, planted with susceptible cv. Crimson Sweet in Brasília, DF, Brazil. Disease incidence (proportion of symptomatic plants) and severity were evaluated separately at four increasing distances from each focus (radius of 50 cm, 150 cm, 250 cm and 350 cm from point sources), 56, 63, 70 and 77 days after planting (DAP). Disease severity evaluations were performed with a 6-class rating scale, ranging from class zero (asymptomatic plants) to disease classes indicating less than 1% blighted leaf area; 1–5% blighted leaf area; 6–25% blighted leaf area; 26–50% blighted leaf area; and more than 50% blighted leaf area. The rating system was adapted from a scale published by the International Centre for Tropical Agriculture (CIAT 1983). At several points during the disease cycle, leaves were collected and the pathogen was re-isolated to confirm the causal agent of observed leaf blight.

GSB progress in watermelon genotypes with distinct levels of resistance

This study was conducted during the rainy season (December 2003 to February 2004), at the Experimental Field Station of Universidade de Brasilia, DF, Brazil, in an area never previously cultivated with cucurbitaceous crops. Progress curves were studied on commercial genotypes Crimson Sweet (susceptible, S) and Riviera (moderately resistant, R) which had their reactions to GSB previously determined (Santos and Café-Filho 2005). Inoculum for initial disease foci consisted of 10 cm length infected watermelon stem segments, freshly collected in a commercial watermelon field, placed next to the crown of two adjacent plants in the center of each plot, 43 DAP. Experimental design was a randomized complete block with four replicates and eight plants *per* plot. Disease incidence was calculated as the proportion of diseased plants and disease severity was estimated using the scale described above. For the construction of disease progress curves and goodness-of-fit calculations, each disease severity note was converted to its respective percent class mid-point (Campbell and Madden 1990), up to season end, at 89 DAP. Presence of *D. bryoniae* in symptomatic lesions was confirmed by optical microscopy during the course of the experiment. Best fit was determined by the adjusted coefficient of determination (R^{*2}), obtained by the linear regression of predicted and calculated values, and by the analysis of residuals distribution (Campbell and Madden 1990).

Gradient models and spatial patterns analysis

Spatial studies of watermelon gummy stem blight epidemics were conducted in the dry season of 2003 (June to September) at the Experimental Field Station of Universidade Federal do Tocantins, TO, Brazil, in an area previously cultivated with rice and without record of cucurbit production. Two fields of 24× 32 m, separated by a 10 m clearing, were planted with cv. Crimson Sweet at a spacing of 2×2 m, resulting in

192 4 m^2 quadrats (Fig. 1). The experiment was supplemented by daily overhead irrigations at dusk, for a period of *c.* 50 min. Disease incidence and severity data were collected in each quadrat, and the means of two fields were used to examine the best fit of gradient models and the spatial patterns. Incidence was calculated as the proportion of symptomatic plants and severity was rated with the disease scale described above. For statistical analysis, disease severity notes were converted to each respective percent class midpoint at 45, 50, 55, 60, 65, 74, 80 and 87 DAP.

Point-source inoculum (*sensu* Madden et al. 2007) at each field was created by inoculation of one plant of the centre row, located at 9 m from the eastern edge at 34 DAP (Fig. 1). Locations closer to the eastern edge were chosen according to the expected prevailing winds. Inoculations were performed with infected watermelon stem segments as described above. Although there was no monitoring for external airborne inoculum, based on the planting history of the Experimental Station and absence of cucurbit fields in the surrounding area, the disease gradients observed subsequently were assumed to be due to disease spread from the artificially created point-sources.

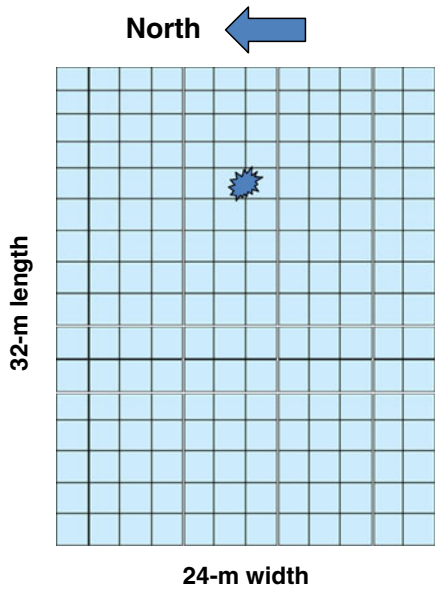

Fig. 1 Diagram of the field experiment for gradient models and spatial pattern analysis. Point-source inoculum was created by inoculation of one central-row plant, 9 m from eastern edge, 34 days after planting. Each of the 192 quadrats are 2×2 m. Explosion mark indicate location of point source inoculum

Isopath maps of watermelon GSB were constructed for each evaluation. The establishment of isopath areas for each evaluation was done using the least squares procedure weighted by distance (SigmaPlot 10) and as data, the matrix of severity in each quadrat. The number of previously selected isopath areas for each evaluation was the same, while the levels of each isopath area were arbitrarily selected, with the purpose of enhancing any possible differences.

Disease gradient regression analysis was done at 74 DAP, separately in the four cardinal directions, by a fitting power law model, $Y=a.s^{-b}$ (Gregory 1968) and an exponential model, $Y=a.e^{(-b.s)}$ (Kiyosawa and Shiyomi 1972). In both models, disease intensity is represented by the 'Y' and distance from the point source is represented by 's'. Parameters 'a' and 'b' indicate source efficiency and rate of disease decline, respectively. Levels of significance for gradient parameters were estimated according to Little and Hills (1978). In addition, GSB aggregation was determined at 74 DAP by the Ordinary Runs procedure (Madden et al. 1982), as described in Campbell and Madden (1990).

Spatial patterns were examined by bi-dimensional spatial correlation (2DCorr) and spatial autocorrelation (LCOR) methods. 2DCorr was used to evaluate relations between quadrats considering presence or absence of GSB symptoms in a given quadrat whereas LCOR was used to assess the severity connection between locations. 2DCorr can be seen as a method to unravel the spatiotemporal dynamics of alloinfections whilst LCOR was used to understand the dynamics of autoinfections.

2DCorr is based on counting pairs of positions (diseased-diseased, diseased-healthy, healthy-diseased and healthy-healthy) in actual experimental maps and comparing them to the expected frequencies in a random spatial pattern (Ferrandino 1998). Binary data matrices (x,y,z) for all evaluations were introduced into the programme and the probability of error of each x,y position was calculated. Based on that, positively correlated lag positions (+lags, $P=0.05$) were marked; the arrangement of significant and non-significant positions is known as the proximity pattern. Row effects were determined for each evaluation considering the number of significant lag distance positions within or across rows that were contiguous with the [0.0] lag position of the proximity pattern.

Severity relationships among quadrats of 2×2 m were examined with spatial autocorrelation analysis

(Gottwald et al. 1992a, b). The spatial position of each quadrat and GSB severity were used as input data. Autocorrelation proximity patterns were generated by registering positively (SL+), negatively and non-correlated lag positions. The size and shape of core clusters of SL + were determined, considering that a core cluster is a group of significant (P=0.05) positively correlated spatial lag positions that form a discrete and contiguous group with the autocorrelation proximity pattern origin (*i.e.*, lag [0.0]). The strength of aggregation is a measure of the core cluster compactness, and it was calculated as (SL + in core clusters/total number of SL+). Edge effects were considered significant if the proportion of SL + at the distal edges of the proximity pattern was in excess of 0.05.

Results

Effect of inoculum source distance on GSB progress in rainfed watermelon

The rainy season in Ponte Alta was extremely favourable to GSB, combining frequent and heavy rains, high temperatures and high relative humidity. Disease started earlier, and maximum disease values were reached sooner at the radial areas adjacent to natural foci (52 cm, Fig. 2). The furthest the distance from a focus, the later was disease onset. However, irrespective of the distance from the source, from 52 to 352 cm, disease incidence and severity within each radius seemed to progress at similar rates (Fig. 2). While the incidence and severity curves displayed analogous trends, incidence reached maximum values (100%) earlier than severity. Final disease records at all radial distances from foci reached destructive levels, abbreviating the expected crop cycle by *c.* 10 days.

GSB progress in watermelon genotypes with distinct levels of resistance

First foliar blight symptoms were observed on cv. Crimson Sweet only 11 days after foci establishment (Fig. 3, 54 DAP), and peaked after two consecutive days of heavy rains that accumulated 135 mm at 59–60 DAP (rain data not shown). A total of 395 mm of rain was recorded between 39 DAP and 88 DAP. Relative humidity was always above 80%, and maximum and minimum temperatures oscillated between 26–31°C and 19–22°C, respectively (not shown). While disease occurred on both genotypes, the disease progress slope was much steeper in Crimson Sweet (S), reaching more than 75% blighted leaves at season end (Fig. 3). In Riviera (R) disease symptoms started later (*c.* 64 DAP) and reached *c.*

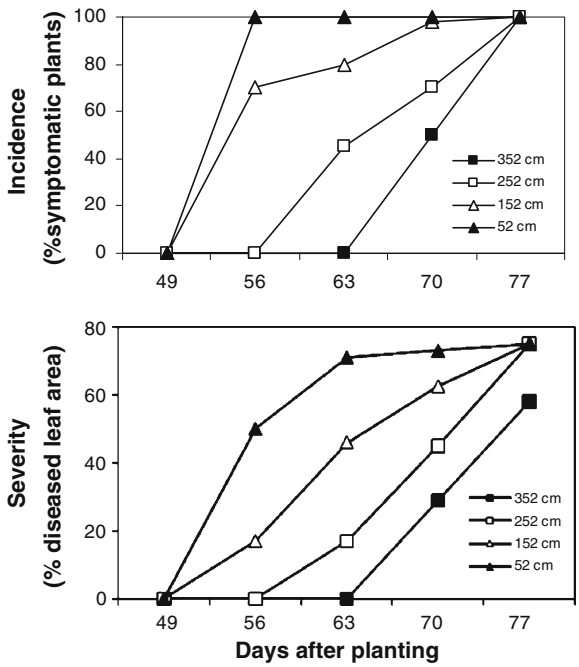

Fig. 2 Incidence and severity progress curves of gummy stem blight at various radial distances from naturally-occurring infection foci in a rainfed watermelon commercial field

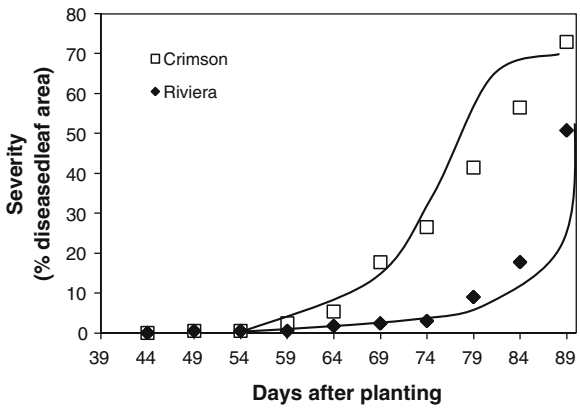

Fig. 3 Progress of gummy stem blight in susceptible cv. Crimson Sweet and partially resistant hybrid Riviera in a rainfed experimental field. Plots were inoculated at 43 days after planting. Some marks represent more than one replicate

50% blighted area. The plot of residues revealed no appreciable trend with the Logistic and Gompertz transformations but the Monomolecular model overestimated disease values in the first half of the season and underestimated on the second half (not shown). When residues were plotted against predicted values (Campbell and Madden 1990) the Gompertz model resulted in a somewhat less scattered distribution than the Logistic model (not shown). Overall, the Gompertz model resulted in the best fit for both genotypes (Table 1, higher adjusted coefficients of determination, R^{*2}). Apparent daily infection rates calculated with the Gompertz model were 0.020 and 0.049 for the resistant and susceptible genotypes respectively (Table 1).

Gradient models and spatial patterns analysis

Watermelon gummy stem blight epidemics were very similar in both replicated areas, and therefore only one area is represented in Fig. 4. No rainfall was recorded after point source inoculum was created. Taken together, the overall shapes of the isopaths (Fig. 4) and of the gradient curves (Fig. 5) support the assumption that all the inoculum was dispersed from the point sources. Even under less than optimal conditions (no rains and 60.8% mean relative humidity) GSB was recorded in all quadrats of the entire 768 m^2 area at 80 DAP. At the beginning and up to 50 DAP, GSB symptoms were only found around the inoculum source. First secondary foci were detected 60 DAP when blighted leaves were found up to 19 m from the inoculum source and the number of such foci increased at 65 and 74 DAP evaluations (Fig. 4). From then on, incidence reached its maximum, while severity intensified progressively. Ordinary runs statistics at 74 DAP were Z (u) −3.38 and −4.12 for each of the two replicated areas, characterizing GSB spatial pattern as non-random or aggregated.

Bi-dimensional spatial correlation (2DCorr) revealed significant + lags contiguous to the [0.0] position of the proximity pattern in all evaluations with the exception of fourth (65 DAP) and the last two (80 and 87 DAP) when quadrat incidence had reached 100%. When present, the core cluster was nearly isodiametric with significant spatial dependencies of one spatial lag (Fig. 4). Significant + lags of higher order were found at 65 and 74 DAP.

Spatial autocorrelation results generally agreed with those of 2Dcorr. Significant + lags were found in every single evaluation, and the severity core cluster was also isodiametric up to one lag distance. Edge effects were detected only at 65 DAP but a higher distance relationship was also found at 87 DAP. The number of significant + lags increased from an average three to 11 at 87 DAP, the final evaluation. The strength of aggregation was high for the experiment´s entire course, reaching its maximum in all but two (65DAP [0.75] and 87 DAP [0.82])) evaluations.

In the analysis of disease gradients at each cardinal direction, the exponential model proved superior to the power law model for either incidence or severity (Table 2). Therefore, disease gradients in each direction are represented by the exponential model (Fig. 5). Source efficiency, represented by parameter 'a' (exponential model) varied by cardinal directions and was higher north- and west-bound and much less efficient in the respective opposite directions (Table 2). This followed the predominant winds.

Discussion

Epidemics developed in different conditions in three locations and over a range of environments, resulting in extremely high disease levels of gummy stem

Table 1 Analysis of gummy stem blight progress curve parameters by three growth models in susceptible (cv. Crimson Sweet) and moderately resistant (Riviera) watermelon genotypes

Disease progress model[a]	Crimson sweet			Riviera		
	Intercept	slope	R^{a2}	intercept	slope	R^{a2}
Monomolecular $y = 1 - [(1 - y_0)\exp(-r.t)]$	-1.5066	0.0280	51	-6.7066	0.0525	25
Logistic $y = 1/[1 + \exp(-\{\ln[y_0/(1 - y_0)]+r.t\})]$	-8.7379	0.1013	84	-0.6528	0.0117	54
Gompertz $y = \exp[\ln(y_0)\exp(-r.t)]$	-3.724	0.0488	96	2.3456	0.0201	95

[a] y = disease values; r = rate of disease progress; t = time;

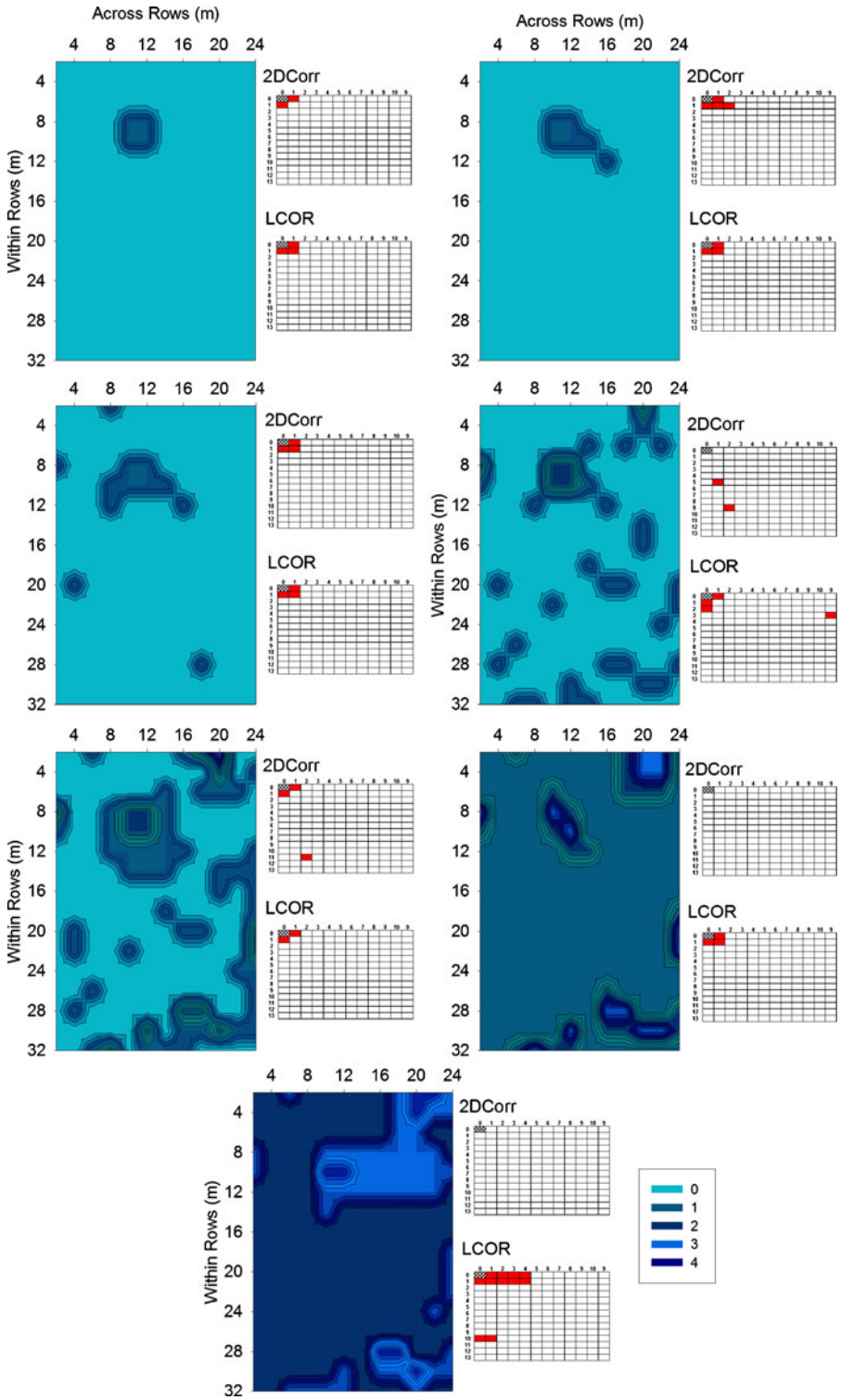

Fig. 4 Isopath maps of watermelon gummy stem blight from point source focus, created 34 days after planting (DAP) and corresponding bidimensional spatial correlation (2DCorr) and spatial autocorrelation (LCOR) graphs. Light blue areas in each isopath represent no symptomatic leaves (Class 0). Class 1 represents less than 1% blighted leaves, Class 2 represent 1–5% , Class 3 represent 6–25% and Class 4 represent 26–50% blighted leaves. Upper left and right: isopaths at 50 and 55 DAP; upper middle left and right: isopaths at 60 and 65 DAP; lower middle left and right: isopaths at 74 and 80 DAP; and bottom: isopath at 87 DAP. Northern direction in all maps is to the left

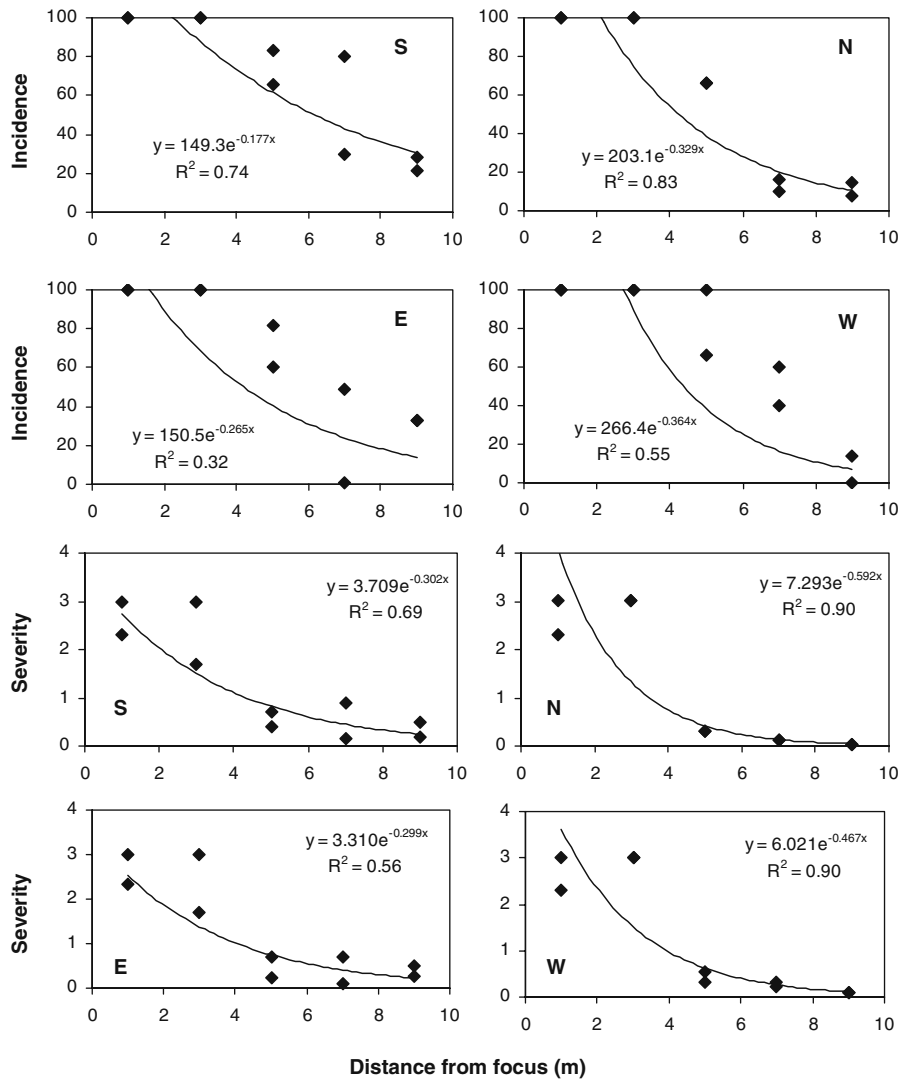

Fig. 5 Gummy stem blight disease gradient curves in overhead irrigated experimental plots planted with a susceptible watermelon cultivar, in the cardinal directions (N, S, E, W)

Table 2 Parameter estimates and coefficients of determination (R^2) for watermelon gummy stem blight incidence and severity by the Power Law and Exponential models, for the four cardinal directions; 'a': source efficiency; 'b' gradient slope, 74 days after planting

Direction	Power Law ($Y=a*s^{-b}$)			Exponential ($Y=a*e^{-b*s}$)		
	a	b	R^2	a	b	R^2
Parameters for Incidence Values[1]						
North	249.21	−0.3231	0.58*	203.09	−0.3291	0.83**
South	137.62	−0.5734	0.54*	149.26	−0.1774	0.74**
East	153.73	−0.9592	0.29 NS	150.54	−0.2653	0.32 NS
West	203.12	−1.1033	0.35 NS	266.40	−0.3642	0.55*
Parameters for Severity Values[1]						
North	0.1382	−1.9790	0.75**	7.2932	−0.5923	0.89**
South	3.5247	−1.0666	0.64**	3.7090	−0.3025	0.69**
East	3.3622	−1.1011	0.58*	3.3103	−0.2986	0.56*
West	4.8549	−1.5577	0.74**	6.0213	−0.4699	0.90**

[1] Not significant (N.S.), or significant at 5% (*) or 1% (**) levels, according to Little and Hills (1978), with 8 degrees of freedom.

blight by the end of each season. It is worth noticing that GSB seemed to progress at similar rates at all radial distances from the foci. Rates were reduced only when intensity values were close to their maximum, an effect of multiple infections within a context of finite healthy tissue at each radius (Vanderplank 1963). The fact that no decrease in the infection rates was observed with distances up to 352 cm from the focus illustrates the efficiency of the initial inoculum sources in natural conditions. The rapid disease progress and high disease levels recorded in a non-inoculated field plainly represent GSB´s highly destructive potential in a commercial field planted with a susceptible cultivar in the rainy season in Central Brazil.

Differences in GSB temporal progress were evident in resistant and susceptible genotypes, but still final disease levels varied from high to destructive (Fig. 3). The Gompertz was earlier indicated as the most appropriate model for polycyclic foliar diseases, based mainly on wheat rust epidemics caused by *Puccinia recondita* (Berger 1981). Our results showed, furthermore, that this model is also superior in the temporal analysis of gummy stem blight, a polycyclic disease with a very different dispersal pattern to that of common rusts (Table 1). The fact that results were consistent for genotypes with different levels of resistance may be regarded as a partial validation of model adjustment. Using the Gompertz model, apparent infection rate (parameter 'r') was 0.020 for the resistant genotype, and more than twice that for the susceptible genotype (0.049). The reduced infection rate in the moderately resistant genotype, coupled with a later onset of disease in the field (*c.* 10 days later than in the susceptible genotype, Fig. 3) resulted in an appreciable reduction in the disease levels at harvest time (about 80 DAP in field conditions). Indeed, a reduction of infection rates usually has a larger impact on final disease levels (and yield) than the reduction of initial inoculum in polycyclic diseases. Crop losses due to GSB in susceptible watermelon cultivars are high (Santos et al. 2005). Although not sufficient for complete disease control in this case, the moderate level of resistance of cv. Riviera is nonetheless a valuable component of disease management.

Even in the dry season and with single and discrete points of inoculum, extremely high disease levels developed. The 100% gummy stem blight incidence close to the season's end (Fig. 4) is especially worth noting. The rapid disease development recorded here may be explained by the choice of a very susceptible cultivar (Santos and Café-Filho 2005), selection of sprinkler irrigation (which causes splash dispersal of fungal propagules), and the timing of irrigation (at dusk), coupled with the occurrence of dew. Differences between the maximum and minimum temperatures in the course of the experiment averaged 18.3°C, and dew was frequently observed in the first morning hours up to 09.00 local time. Gummy stem blight´s spatial pattern was characterized as aggregated for both incidence and severity and for most evaluations a short distance but strong spatial dependency was detected. In fact, the early isopaths (50 and 55 DAP) point to infection from quadrat to neighbouring quadrat only (autoinfection). This pattern is generally consistent with pycnidial fungi, such as those represented by the anamorphic phase of the causal agent, *Ascochyta cucumis*, and other splash-dispersed fungi (Tu 1981; Laranjeira et al. 1998; Pinto et al. 2001).

However, the spatial relationship observed between 60 and 74 DAP indicates that concurrence of ascospores of teleomorphic phase (*Didymella bryoniae*) in the epidemics cannot be ruled out as responsible for the establishment of secondary foci (Schenck 1968; Fig. 4). Ascospores of *Didymella bryoniae* are mainly air-dispersed and have a greater tendency to be diluted and escape the canopy than the conidia of the anamorphic phase. Indeed, the isopaths at 60 DAP and after clearly show a wave of alloinfections (putatively due to the wind-dispersed ascospores). Although these alloinfections could be the result of airborne inoculum external to the experimental field, we assumed that all or most of these infections are from field-borne ascospores, based on the planting history of the Experimental Station and absence of cucurbit fields in the surrounding area. In addition, GBS is a polycyclic disease and secondary cycles with concurrent formation of pycniospores and ascospores have been noted during the progress of GBS epidemics in commercial watermelon fields in Brazil (Santos and Café-Filho 2006).

Clearly, source efficiency was higher in the north and western directions (Table 2), and much less efficient in the opposite directions. All water droplets were due to the water splash from the overhead irrigation system, since no rains were recorded after the creation of point sources, at 34 DAP. This is also consistent with the fact that splashed spores are carried preferentially in the

direction of the observed prevailing winds, even though no formal wind records are available for the study period. Disease also decreased faster (more negative 'b' values) in the north and western directions, probably a consequence of the initially very aggregated disease pattern, due to the relatively small distances travelled by the inoculum (in the form of conidia) at each dispersion event (irrigation). In fact, according to Aylor (1987), the exponential model stresses deposition incidents in the dispersion process while the power law model emphasizes dilution incidents. Given the distances examined (up to 9 m), it is believed that the deposition effects derived from irrigation events governed the dynamics of dispersion and, consequently, disease gradients were well represented by the exponential model. Furthermore, earlier measurements of *D. bryoniae* isolates found pycniospores and ascospores of average lengths of 11.6 μm and 13.7 μm respectively (Santos and Café-Filho 2006). These spore sizes are within the range given by Fitt and Bainbridge (1984) and Grove et al. (1985) for splash-dispersed pathogens better represented by the exponential model, while dispersions of pathogens with spores shorter than 10 μm are usually best described by the power law model. Freitas et al. (1998) and Pinto et al. (2001) also found best goodness-of-fit with the exponential model to describe soybean stem canker (*Diaporthe phaseolorum* f.sp. *meridionalis*) and bean anthracnose (*Colletotrichum lindemuthianum*) disease gradients, both caused by splash-dispersed pathogens.

The temporal and spatial dynamics epidemics of watermelon gummy stem blight epidemics described in commercial and experimental fields are consistent with epidemics of polycyclic diseases that are mainly dependent on splash-dispersed spores. Patterns were consistent in different localities, climates, irrigation systems and host genotypes, and overall point out GSB's highly destructive potential even when starting from relatively small, localized sources. In addition, the value of partial genetic resistance as a component of disease management was determined quantitatively: the slope of disease progress curves of partially resistant and susceptible genotypes may be useful for selection of disease management practices.

Acknowledgements Research funded by the Brazilian National Research Council (CNPq), Grant no. 306968/2006-1. A.C. Café-Filho is a CNPq Research Fellow, Grant no. 301095/2009-4.

References

Aylor, D. E. (1987). Deposition gradients of urediniospores of *Puccinia recondita* near a source. *Phytopathology, 77*, 1442–1448.

Berger, R. D. (1981). Comparison of the Gompertz and logistic equations to describe plant disease progress. *Phytopathology, 71*, 716–719.

Berger, R. D., & Luke, H. H. (1979). Spatial and temporal spread of oat crown rust. *Phytopathology, 69*, 1199–1201.

Campbell, C. L., & Madden, L. V. (1990). *Introduction to plant disease epidemiology* (p. 532). New York: John Wiley & Sons.

CIAT (Centro Internacional de Agricultura Tropical). (1983). *Sistema de evaluación estándar para arroz* (2nd ed., p. 61). Cali: CIAT.

Fajardo, T. V. M., Lopes, C. A., Silva, W. L. C., & Ávila, A. C. (1997). Disseminação da doença e redução da produção em tomateiro industrial infectado por Tospovirus no Distrito Federal. *Fitopatologia Brasileira, 22*, 413–418.

Ferrandino, F. J. (1998). Past nonrandomness and aggregation to spatial correlation: 2DCORR, a new approach for discrete data. *Phytopathology, 88*, 84–91.

Fitt, B. D. L., & Bainbridge, A. (1984). Effect of celulose xanthate on splash dispersal of *Pseudocercosporella herpotrichoides* spores. *Transactions of the British Mycological Society, 82*, 570–571.

Freitas, M. A., Café-Filho, A. C., & Nasser, L. C. B. (1998). Gradientes do cancro da haste da soja (*Diaporthe phaseolorum* f.sp. *meridionalis)* a partir de foco pontual de inóculo. *Fitopatologia Brasileira, 23*, 161–165.

Gottwald, T. R., & Graham, J. H. (1990). Spatial pattern analysis of epidemics of citrus bacterial spot in Florida citrus nurseries. *Phytopathology, 80*, 181–190.

Gottwald, T. R., Reynolds, K. M., Campbell, C. L., & Timmer, L. W. (1992a). Spatial and spatiotemporal autocorrelation analysis of citrus canker epidemics in citrus nurseries and groves in Argentina. *Phytopathology, 82*, 843–51.

Gottwald, T. R., Richie, S. M., & Campbell, C. L. (1992b). LCOR2-Spatial correlation analysis software for the personal computer. *Plant Disease, 76*, 213–215.

Gregory, P. H. (1968). Interpreting plant disease dispersal gradients. *Annual Review of Phytopathology, 6*, 189–212.

Grove, G. G., Madden, L. V., & Ellis, M. A. (1985). Splash dispersal of *Phytophthora cactorum* from infected strawberry fruit. *Phytopathology, 75*, 611–615.

Keinath, A. P. (1995). Fungicide timing for optimum management of gummy stem blight epidemics on watermelon. *Plant Disease, 79*, 354–358.

Keinath, A. P. & Duthie, I. A. (1998). Yield and quality reductions in watermelon due to anthracnose, gummy stem blight and black rot. p.77–90. In Anonymous. *Recent research developments in plant pathology* **2**, Research Signpost, Trivandrum, India.

Keinath, A. P., May, W. H., & Dubose, V. B. (1997). Comparison of eight fungicide intervals to control gummy stem blight on watermelon. *Fungicide and Nematicide Tests, 52*, 195.

Kiyosawa, S., & Shiyomi, M. (1972). A theoretical evaluation of the effect of mixing resistant variety with suscetible

variety for controlling plant diseases. *Annals of the Phytopathological Society of Japan, 38*, 41–51.

Laranjeira, F. F., Amorim, L., Bergamin-Filho, A., Berger, R. D., & Hau, B. (1998). Análise espacial do amarelecimento fatal do dendezeiro para elucidar sua etiologia. *Fitopatologia Brasileira, 23*, 397–403.

Little, T. M., & Hills, F. J. (1978). *Agricultural experimentation, design and analysis*. New York: J. Wiley & Sons.

Madden, L. V., & Hughes, G. (1995). Plant disease incidence, distribution, heterogenicity and temporal analysis. *Annual Review of Phytopathology, 33*, 529–564.

Madden, L. V., Louie, R., Abt, J. J., & Knoke, J. K. (1982). Evaluation of tests for randomness of infected plants. *Phytopathology, 72*, 195–198.

Madden, L. V., Hughes, G., & van den Bosch, F. (2007). *The study of plant disease epidemics*. St Paul: APS.

Maffia, L. A., & Berger, R. D. (1999). Models of plant disease epidemics. II: Gradients of bean rust. *Journal of Phytopathology, 147*, 199–206.

Pinto, A. C. S., Pozza, E. A., Talamini, V., Machado, J. C., Sales, N. L. P., Garcia-Júnior, D., et al. (2001). Análise do padrão espacial e do gradiente da antracnose do feijoeiro em duas épocas de cultivo. *Summa Phytopathologica, 27*, 392–398.

Santos, G. R., & Café-Filho, A. C. (2005). Reação de genótipos de melancia ao crestamento gomoso do caule. *Horticultura Brasileira, 23*, 945–950.

Santos, G. R., & Café-Filho, A. C. (2006). Ocorrência do crestamento gomoso do caule em melancia no Tocantins causado por *Didymella bryoniae*. *Fitopatologia Brasileira, 31*, 208.

Santos, G. R., Café-Filho, A. C., Leão, F. F., César, M., & Fernandes, L. E. (2005). Progresso do crestamento gomoso e perdas na cultura da melancia. *Horticultura Brasileira, 23*, 228–232.

Schenck, N. C. (1968). Epidemiology of gummy stem blight (*Mycosphaerella citrulina*) on watermelon: ascospore incidence and disease development. *Phytopathology, 58*, 1420–1422.

Tu, J. C. (1981). Antracnose (*Colletotrichum lindemuthianum* L.) in southern Ontario: spread of disease from an infection focus. *Plant Disease, 65*, 477–480.

Vanderplank, J. E. (1963). *Plant diseases: Epidemics and control*. New York: Academic.